

Rational Design of Azo-Azomethine Receptors for Sensing of Inorganic Fluoride: Construction of Molecular Logic Gates and DFT Study

Hamid Khanmohammadi,^{A,B} Khatereh Rezaeian,^A
and Nafiseh Shabani^A

^ADepartment of Chemistry, Faculty of Science, Arak University, Arak 38156-8-8349, Iran.

^BCorresponding author. Email: h-khanmohammadi@araku.ac.ir

New azo-azomethine receptors, **HL**ⁿ ($n = 1-3$), have been synthesised via condensation reaction of 5-(4-X-phenyl)-azo-salicylaldehyde ($X = \text{NO}_2, \text{Cl}$ and CH_3) with (4-nitrobenzylidene)hydrazine. The receptor with a *p*-NO₂ substituent on the aromatic ring of the azo moiety (**HL**¹) has excellent sensitivity and selectivity towards basic anions with proper discrimination between F⁻ and AcO⁻ or H₂PO₄⁻ in DMSO–water (4 : 1). A Job's plot displays a 1 : 1 stoichiometry between **HL**¹ and F⁻ alone with a detection limit of 0.737 μM for fluoride ions. The solvatochromic behaviour of **HL**¹ was probed by studying its UV-vis spectra in four pure organic solvents of different polarities and a meaningful correlation was observed. Furthermore, **HL**¹ was used for detection of inorganic fluoride in toothpaste. The systematic density functional theory (DFT) and time dependent-DFT calculations have been carried out to investigate the mechanism of colourimetric sensing of fluoride ion by **HL**¹ in the gas phase and in solution. Moreover, by using F⁻ and H⁺ as chemical inputs, and the absorbance as output, a INHIBIT logic gate was constructed, which exhibits 'Write–Read–Erase–Read' ability without obvious degradation in its optical output.

Manuscript received: 7 June 2017.

Manuscript accepted: 29 June 2017.

Published online: 10 August 2017.

Introduction

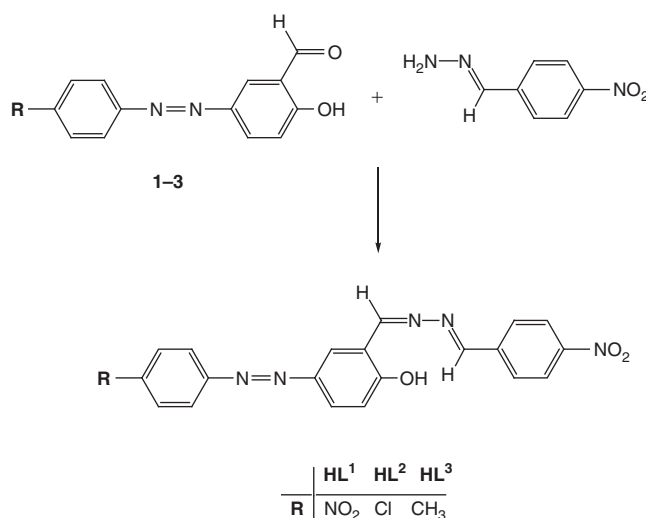
In recent years, the development of artificial receptors for recognition and colourimetric sensing of biologically important anions has gained much significance.^[1–3] For this purpose several chemoreceptors have been designed and evaluated for naked eye detection of various anions without resorting to any expensive spectroscopic instruments.^[4,5] On the other hand, recently, much attention has been paid to the synthesis and use of Schiff base receptors, as privileged chemosensors which can be easily prepared, for naked eye detection of anions in organic, aqueous, and semi-aqueous media.^[6–8]

Among the biologically important anions, F⁻ is of particular interest owing to its established role in biological systems and in our life.^[9–11] For instance, fluoride ions are especially useful in the treatment of osteoporosis, dental care, drinking water quality control, and detection of chemical warfare agents. However, high doses of fluoride ions cause skeletal fluorosis, thyroid activity depression, bone disorders, and immune system disruption.^[12,13] Besides the above emphasis, the detection of fluoride ions by using simple preparation and minimal instrumental assistance is desirable towards practical applications.^[14,15] To date several receptors with amide, urea, thiourea, amidourea, pyrrole, imidazolium, and indole moieties have been reported which are capable to detect fluoride ions with high affinity.^[16,17] Nevertheless, in most cases, the reported receptors are considerably expensive and difficult to prepare.^[18] Particular interest in this regard is inexpensive colourimetric sensing, which would

allow naked eye detection of fluoride in an easy way. It is always preferable to have potential hydrogen bond donor groups, such as –OH or –NH, in chemosensors, which in turn can increase the attraction of the sensor towards F⁻ via highly dissociable protons.^[19,20] Accordingly, highly sensitive and easy-to-prepare salicylaldehyde-based Schiff base colourimetric receptors, which are regarded as the hydrogen donors to form real hydrogen bonds between fluoride ions and corresponding receptors R–O–H⋯F⁻, have become particularly attractive.^[21,22]

Moreover, chemosensors based on colourimetric receptors can be further explored for the construction of molecular devices such as molecular logic gates, switches, diodes, wires, and molecular keypads.^[23] In this context, Boolean logic gates are considered advanced microdevices capable of performing binary arithmetic and logical operations based on molecules.^[7,24,25] These systems are believed to alter the chemically encoded information as input into optical changes as readable output signals, leading to the development of molecular logic gates such as AND, OR, XOR, NAND, NOR, and INHIBIT logic gates.^[26–28] During the past years, extensive investigations have been devoted towards integrated logic gates such as INHIBIT, half-adder and half-subtractor with single receptors.^[29]

In pursuit of these, we have designed and synthesised new azo-azomethine based colourimetric receptors, **HL**ⁿ ($n = 1-3$) (Scheme 1). The prepared receptors were characterised using spectroscopic methods (FT-IR, UV-vis, and ¹H NMR) as well as elemental analysis data. The sensing ability of the receptors



Scheme 1. Azo-azomethine receptors, HL^n ($n = 1-3$).

towards various anions (such as F^- , Cl^- , Br^- , AcO^- , I^- , H_2PO_4^- , N_3^- , NO_2^- , NO_3^- , and HSO_4^- as their tetrabutylammonium (TBA) salts) has been investigated. In these circumstances, all receptors sense the more basic anions such as F^- , AcO^- , and H_2PO_4^- . However, it was observed that HL^1 , with a *p*- NO_2 substituent on the aromatic ring of the azo moiety, has excellent sensitivity and selectivity towards basic anions with proper discrimination between F^- and AcO^- or H_2PO_4^- in DMSO–water (4 : 1). Furthermore, the recognition details of F^- sensing were evaluated using UV-vis spectroscopy and time-dependent density functional theory (TD-DFT) methods. The molecular structure of HL^1 has been optimised at the standard level of theory. The energies of the highest occupied molecular orbitals and lowest unoccupied molecular orbitals (HOMO and LUMO) of the energetically stable tautomer, enol–amine, were also obtained, before and after reaction with fluoride ions, in the gas phase and in solution. The result indicated that the energy gap between the HOMO and LUMO of HL^1 decreased in the presence of fluoride ions due to complex formation.

Moreover, the remarkable UV-vis spectroscopic responses of HL^1 in DMSO towards fluoride ions and protons, as external chemical stimuli, inspired us to design circuits for electronic devices (i.e. molecular logic gates). Accordingly, the potential circumstances provide opportunities for HL^1 to mimic the INHIBIT (integrated by combining a NOT, a YES, and an AND gate) and IMP gates using H^+ and F^- as chemical inputs, and monitoring absorbance as output. More interestingly, the spectroscopic responses as well as the colour change can be switched back and forth by successive addition of F^- and trifluoroacetic acid (TFA), as a proton donor, and which may be depicted by a complementary 'IMP/INH' molecular logic gate. Furthermore, based on this reversible and reproducible switching behaviour, a potential 'Write–Read–Erase–Read' memory function possessing a 'Multi-Write' ability has been proposed.

Experimental

Materials

All of the reagents and solvents involved in the synthesis were of analytical grade and used as received without further purification. 4-Nitrobenzaldehyde, 4-nitroaniline, 4-chloroaniline, and

4-methylaniline were obtained from either Aldrich or Merck. Azo-coupled precursors, **1–3**, were prepared as described previously.^[30]

Instrumentation

^1H NMR spectra were recorded on a Bruker Avance 300 MHz spectrometer. FT-IR spectra were recorded as a pressed KBr disc, using a Unicam Galaxy Series FT-IR 5000 spectrophotometer in the region of 400–4000 cm^{-1} . Melting points were determined on an Electrothermal 9200 apparatus. Electronic spectroscopic measurements were carried out using an Optizen 3220 UV in the range 200–700 nm. C, H, and N, analyses were performed on a Vario EL III elemental analyzer.

Computational Study

Computational studies were carried out using the *Gaussian 09* software package.^[31] The starting structure for DFT calculations was prepared using the *GaussView* package.^[32] Each prepared compound's structure was fully optimised using the B3LYP/6–311G (p, d) level of theory.^[33,34] The solute–solvent interactions were calculated using the polarisable continuum model (PCM).^[35] Visualisation of the UV-vis spectra of the receptors and their complexes was carried out using the *Chemission* program <http://www.chemission.com>.

Synthesis

Synthesis of (4-Nitrobenzylidene)hydrazine **1**

The mono-iminated precursor was prepared according to a modified previously reported method.^[36] A solution of 4-nitrobenzaldehyde (1.51 g, 1 mmol) in 10 mL of EtOH was added dropwise, at room temperature, to a solution of N_2H_4 (0.10 g, 3.12 mmol) in 20 mL of EtOH over a period of 1 h with stirring. After the addition was complete, the mixture was kept in a refrigerator for 24 h. The formed solid was collected by filtration, washed with diethyl ether, recrystallised in EtOH, and dried at room temperature. Yield: 1.0 g (60% based on 4-nitrobenzaldehyde), mp 146–148°C. δ (DMSO- d_6 , 300 MHz, ppm) 7.51 (s, 2H), 7.66 (d, 2H, *J* 8.50), 7.74 (s, 1H), 8.15 (d, 2H, *J* 8.50). ν_{max} (KBr)/ cm^{-1} 3424 (NH_2), 1630 (C=N), 1578 (C=C), 1507 (NO_2), 1327 (NO_2), 1103 and 841.

General Procedure for the Synthesis of Azo-Azomethine Receptors, **HL**¹–**HL**³

A solution of (4-nitrobenzylidene)hydrazine (**I**) (0.165 g, 1 mmol) in 10 mL of absolute EtOH was added with stirring to a solution of azo-coupled precursors **1–3** (1 mmol) in 50 mL of absolute EtOH during a period of 10 min at 60°C. The solution was heated in a water bath for 12 h at 80°C with stirring. The mixture was filtered while hot and the obtained solid was washed with hot EtOH (three times) and then with diethyl ether. The resultant product was dried in air.

1-(4-(Hydrazonomethyl)phenyl)-2-(4-nitrophenyl)diazene (HL¹). Orange solid. Yield: 95 %, mp 257–259°C. δ_{H} (DMSO-*d*₆, 300 MHz) 7.22 (d, 1H, *J* 8.79), 8.07 (m, 5H), 8.41 (m, 5H), 8.98 (s, 1H), 9.10 (s, 1H), 11.94 (b, 1H). δ_{C} (DMSO-*d*₆, 300 MHz) 152.2, 124.6, 123.2, 160.8, 144.7, 123.9, 126.7, 116.0, 166.3, 118.4, 147.1, 146.4, 135.9, 128.1, 124.0, 149.2. ν_{max} (KBr)/cm⁻¹ 1628 (C=N), 1603 (C=C), 1518 (NO₂), 1460 (N=N), 1341 (NO₂), 1277, 1107, 854. λ_{max} (DMSO)/nm (ϵ /M⁻¹ cm⁻¹) 280 (26933), 355 (41633), 395 (42233). *m/z* 122.0, 149.1, 269.2 (molecular ion peak was not observed: [M]⁺ = 417.1). Anal. Calc. for C₂₀H₁₄N₆O₅: C 57.42, H 3.37, N 20.09. Found: C 57.10, H 3.22, N 20.31 %.

1-(4-(Hydrazonomethyl)phenyl)-2-(4-chlorophenyl)diazene (HL²). Yellow solid. Yield: 90 %, mp > 300°C. δ_{H} (DMSO-*d*₆, 300 MHz) 7.18 (m, 2H), 7.67 (m, 1H), 7.88 (d, 4H, *J* 7.93), 8.16 (d, 4H, *J* 8.46), 9.11 (s, 2H), 11.80 (br, 1H). δ_{C} (DMSO-*d*₆, 300 MHz) 137.1, 126.4, 122.2, 152.1, 141.7, 123.2, 127.1, 116.1, 164.3, 118.3, 145.1, 146.4, 135.9, 128.1, 124.0, 149.2. ν_{max} (KBr)/cm⁻¹ 1630 (C=N), 1576, 1481 (N=N), 1400, 1313 (NO₂), 1277, 1196, 837, 743. λ_{max} (DMSO)/nm (ϵ /M⁻¹ cm⁻¹) 263 (11500), 348 (34366) in DMSO. *m/z* 111.0, 122.0, 149.1, 258.7 (molecular ion peak was not observed: [M]⁺ = 407.0). Anal. Calc. for C₂₀H₁₄ClN₅O₃: C 58.90, H 3.46, N 17.17. Found: C 58.77, H 3.60, N 17.35 %.

1-(4-(Hydrazonomethyl)phenyl)-2-(4-methylphenyl)diazene (HL³). Yellow solid. Yield: 95 %, mp 238–240°C. δ_{H} (DMSO-*d*₆, 300 MHz) 2.40 (s, 3H), 7.16 (d, 1H, *J* 8.79), 7.39 (d, 2H, *J* 7.93), 7.78 (d, 2H, *J* 7.93), 7.97 (d, 1H, *J* 11.65), 8.15 (d, 2H, *J* 8.43), 8.36 (m, 3H), 8.98 (s, 1H), 9.10 (s, 1H) 11.73 (br, 1H). δ_{C} (DMSO-*d*₆, 300 MHz) 24.1, 139.2, 128.4, 122.9, 147.1, 140.7, 123.1, 126.1, 116.1, 163.3, 118.2, 145.1, 146.4, 135.9, 128.1, 124.0, 149.2. ν_{max} (KBr)/cm⁻¹ 1632 (C=N), 1603 (C=C), 1522 (NO₂), 1489 (N=N), 1341 (NO₂), 1279, 1109, 843. λ_{max} (DMSO)/nm (ϵ /M⁻¹ cm⁻¹) 250 (1633), 345 (43100). *m/z* 911.0, 122.0, 149.1, 238.0 (molecular ion peak was not observed: [M]⁺ = 387.1). Anal. Calc. for C₂₁H₁₇N₅O₃: C 65.11, H 4.42, N 18.08. Found: C 64.90, H 4.50, N 18.19 %.

Results and Discussion

Synthesis

The azo-azomethine receptors **HL**^{*n*} (*n* = 1–3), were obtained by the condensation reaction of azo-coupled precursors **1–3** with (4-nitrobenzylidene)hydrazine (**I**) in EtOH (Scheme 1). The compounds were fully characterised using IR and NMR spectroscopy as well as microanalytical data (Supplementary Material). The total absence of the $\nu(\text{C}=\text{O})$ absorption band of the azo-coupled precursors in the IR spectra at 1666–1668 cm⁻¹ together with the appearance of a new absorption band at 1628–1632 cm⁻¹ obviously indicate that the new azo-azomethines were formed (Table 1).^[37,38] In the ¹H NMR spectra of **HL**^{*n*} (*n* = 1–3), the CH=N protons appear as two singlet resonances at 8.90–9.98 ppm (Supplementary Material). The broad signal at 11.50–12.00 ppm was assigned to the OH proton, as was confirmed by deuterium exchange when D₂O was added to a DMSO-*d*₆ solution of **HL**^{*n*} (*n* = 1–3).

The Electronic Absorption Spectra: Substituent Effect

The electronic absorption spectra data of the azo-coupled precursors and their related azo-azomethine receptors, recorded in DMSO at room temperature, are given in Table 1.

The electronic absorption spectra of **HL**^{*n*} (*n* = 1–3), in DMSO, mainly display two or three bands (Supplementary Material). The first UV band located at 245–280 nm can be assigned to the moderate energy ($\pi \rightarrow \pi^*$) transition of the aromatic rings while the second band at ~350 nm is due to the low energy ($\pi \rightarrow \pi^*$) transition involving the π -electrons of the azo and azomethine groups.^[39] It can be found that the maximum absorption band, at ~340 nm, slightly shifted bathochromically along with the increase in the electron-accepting ability of substituents in the sequence of **HL**¹ > **HL**² > **HL**³, consistent with an increase in molecular donor–acceptor polarisation (Table 1).^[40] The electronic absorption spectrum of **HL**¹, recorded in DMSO at room temperature, displays another intense band at ~395 nm, due to charge transfer transitions involving the whole molecule of the receptor (Supplementary Material).^[40]

Anion Sensing Study

To provide fundamental insights into the suitability of the prepared receptors as colourimetric anion sensors, the anion sensing behaviour was first evaluated qualitatively by visual examination of the colour changes of a DMSO solution of the receptors after addition of anions, such as F⁻, Cl⁻, Br⁻, AcO⁻, I⁻, H₂PO₄⁻, N₃⁻, NO₂⁻, NO₃⁻, and HSO₄⁻ as their tetrabutylammonium (TBA) salts. The anion recognition behaviour of the current

Table 1. Tentative assignments of some selected IR frequencies and UV-vis data of the prepared azo-azomethine dyes and their azo precursors

Compound	IR frequency ^A [cm ⁻¹]						λ_{max} [nm] (ϵ [M ⁻¹ cm ⁻¹]) in DMSO	
	$\nu(\text{C}-\text{O})$	$\nu(\text{C}=\text{O})$	$\nu(\text{C}=\text{C})$	$\nu(\text{C}=\text{N})$	$\nu(\text{NO}_2)$	$\nu(\text{NH}_2)$		$\nu(\text{N}=\text{N})$
1	1288	1666	1608	—	1525, 1346	—	1479	246 (4500), 382(12700), 551 (1850)
2	1286	1668	1622	—	—	—	1477	256 (6490), 410 (7850), 466(9345)
3	1287	1668	1620	—	—	—	1481	260 (7580), 344 (23400), 437 (3720)
I	—	—	1578	1630	1507, 1327	3424	—	—
HL ¹	1277	—	1603	1628	1518, 1341	—	1479	280 (26933), 355 (41633), 395 (42233)
HL ²	1279	—	1597	1630	1524, 1346	—	1483	263 (11500), 348 (34366)
HL ³	1270	—	1605	1632	1522, 1341	—	1489	250 (1633), 345 (43100)

^AKBr discs.

receptors in DMSO was explored using UV-vis spectroscopy upon the addition of 10 equiv. of the anions. Detailed spectroscopic studies revealed that the addition of the relatively basic anions such as F^- , AcO^- , and $H_2PO_4^-$ elicited marked responses in the electronic spectra of HL^n ($n = 1-3$) whereas weakly basic anions failed to cause any conspicuous spectroscopic changes (Supplementary Material). It has been postulated that among three of the commonly basic anions tested, fluoride and acetate with a higher basicity are anticipated to form strong complexes with sensors and consequently exhibited remarkable spectroscopic changes.

From the viewpoint of practical applications of anion sensors, it is crucial that the probes operate in water-containing media. This objective can be accomplished utilising the sensor decorated by electron-withdrawing substituents to detect anions through the deprotonation mechanism.^[22] Hence, to evaluate the practicability of the sensors in an aqueous environment, we monitored the UV-vis spectra of HL^n ($n = 1-3$) with increasing water content, from 9 : 1 to 4 : 1 DMSO–water solutions. HL^1 was found to be tolerant to the presence of water under 4 : 1 DMSO–water conditions and evidenced good selectivity for fluoride over acetate since it showed a higher extinction coefficient with F^- than that obtained with AcO^- . Surprisingly, the addition of $H_2PO_4^-$, as one of the basic anions, did not induce colour and spectroscopic changes. Accordingly, it is worth noting that HL^1 is capable of allowing a rough discrimination of the three common basic anions (F^- , AcO^- , and $H_2PO_4^-$). These spectroscopic changes also provided colourimetric changes from light yellow to dark blue which can be visually recognised. In contrast to HL^1 , the HL^2 and HL^3 receptors exhibited minor spectroscopic changes on addition of basic anions in a 4 : 1 DMSO–water solution. The above observation can be ascribed to the fact that the introduction of another electron-withdrawing (NO_2) group into the backbone of the molecular sensor augments the acidity of active sites. Therefore the receptor HL^1 is able to compete with water to sense a trace amount of the basic anions.^[41,42]

Encouraged by the favourable features of the sensory system, we employed HL^1 as a colourimetric sensor for practical purposes and to detect fluoride ions in an aqueous environment. To gain a deeper insight into the binding characteristics of sensor HL^1 , UV-vis spectroscopic titrations were performed upon the addition of standard solutions of F^- as its TBA salt to HL^1 ($3 \times 10^{-5} \text{ mol L}^{-1}$) in a 4 : 1 DMSO–water solution. As depicted in Fig. 1, on an incremental increase of F^- , the band

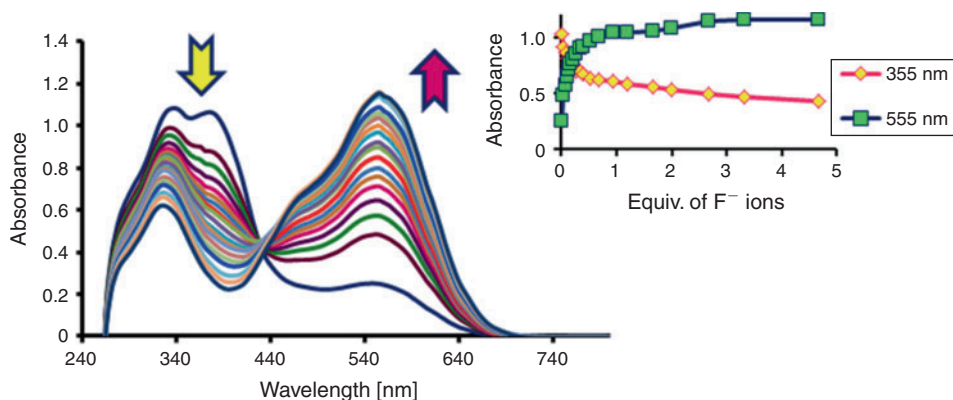


Fig. 1. UV-Vis titration of HL^1 ($3 \times 10^{-5} \text{ mol L}^{-1}$) in 4 : 1 DMSO–water solution with incremental addition of TBAF. Inset shows the binding isotherms at selected wavelengths.

centred at $\sim 355 \text{ nm}$, ascribed to the $\pi \rightarrow \pi^*$ transition of the chromophores, decreased and simultaneously the band at $\sim 600 \text{ nm}$, attributed to the charge transfer and interaction between the fluoride ion and receptor, appeared and developed remarkably with a distinct isosbestic point at 434 nm . These observations were in accordance with the dramatic colour change from yellow to dark blue. Moreover, the Benesi–Hildebrand plot^[43] of $1/[A - A_0]$ versus $1/[F^-]$ for titration of HL^1 with anionic guests provided a straight line (Fig. 2), corroborating the 1 : 1 ratio between HL^1 with a deprotonation constant of $2.74 \times 10^5 \text{ M}^{-1}$ towards F^- . The stoichiometry of the host–guest interaction was also authenticated by use of continuous-variation plots (Job's plots) (Fig. 3). Interestingly, the current system can detect F^- at a low limit of $\sim 7.37 \times 10^{-7} \text{ M}$.

Proton NMR Spectra

In the next step, to shed light on the nature of the interaction between receptor HL^1 and fluoride, 1H NMR titration experiments were conducted. Fig. 4 displays the 1H NMR spectra of HL^1 with different amounts of TBAF in DMSO- d_6 . The 1H NMR spectrum of the free receptor exhibited a broad signal at 11.94 ppm , assigned to the phenolic OH proton, as was authenticated by a D_2O exchange experiment. Interestingly, as expected, the OH proton of the azo phenol entirely vanished, reflecting deprotonation when 1 equiv. of F^- was added into the DMSO- d_6 solution of HL^1 . Simultaneously, all aromatic and azomethine proton signals underwent a continuous upfield shift. The profound upfield shift is attributed to the considerable

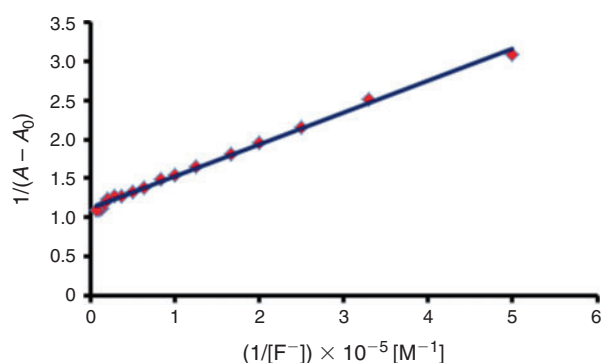


Fig. 2. Benesi–Hildebrand plot of sensor HL^1 binding with F^- anion associated with an absorbance change at 555 nm in 4 : 1 DMSO–water.

augmentation of electron density on to the π -conjugated framework brought by neat OH deprotonation.^[22,44] In addition, a new triplet at 16.1 ppm ($^1J_{\text{HF}} \sim 121$ Hz) appeared which is precisely ascribed to the FHF^- dimer. The generation of FHF^- supports the supposition of the deprotonation event.

Solvatochromic Study

To our delight, upon the addition of 1 equiv. of F^- ions to a HL^1 solution in dry DMSO (3×10^{-5} M), a colour change from yellow to dark blue was observed. This dissimilarity in colour change (yellow to dark blue in DMSO and yellow to red in dioxane) can be attributed to the solvatochromic effect of HL^1 . Surprisingly, this study was further extended to other aprotic solvents such as DMF and acetonitrile where the receptor HL^1 revealed different colouration and spectra only in the presence of F^- ions with respect to the solvent polarity (Fig. 5).

It is worth mentioning that the addition of F^- ions to the receptor solutions induced charge separation. Since HL^1 attains different dipole moments in its ground and lower energy singlet

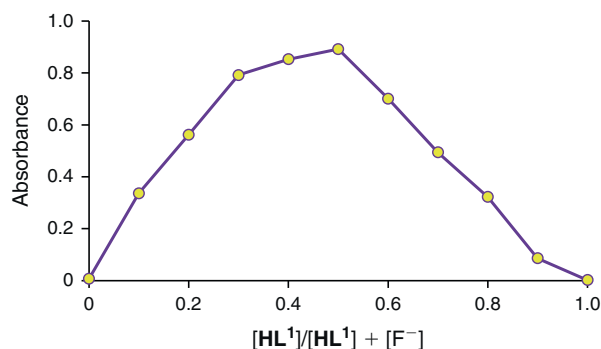


Fig. 3. Job's plot for sensor HL^1 with tetrabutylammonium fluoride using UV-vis spectroscopy.

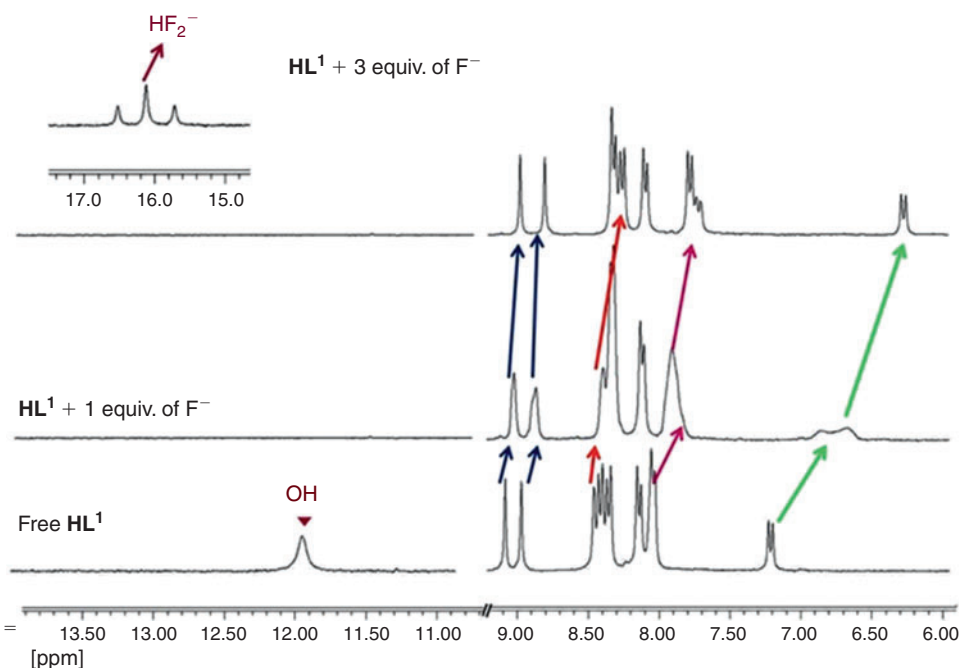


Fig. 4. ^1H NMR spectra of HL^1 in $\text{DMSO}-d_6$ (2×10^{-2} mol L^{-1}) in the absence and in the presence of different amounts of TBAF.

excited state, a charge transfer transition will be established. As a result, interactions between newly established dipole moments and solvent dipole moments will be formed. Eventually, the energy levels of the receptor change with solvent polarity. As the polarity of the solvent increases, these energy levels decrease. Hence, with increasing solvent polarity, the bands corresponding to charge transfer (CT) transitions show a bathochromic shift (positive solvatochromism).^[45] This positive solvatochromism was compared with the dielectric constant of solvents which is depicted in Table 2.^[44] The polarity of the solvent is related to the dielectric constant. The greater the dielectric constant, the greater the polarity and as a result with the increasing dielectric constant the red-shift was expected. This colourimetric discrimination in different solvents was successfully applied to determine the percentage composition of a binary solvent mixture.

Detection of F^- in Toothpaste

In order to examine the potential applicability of HL^1 , a sample containing commercial toothpaste was used for F^- detection. The prepared sample consisted of 0.05 mg mL^{-1} of toothpaste (Crest brand), 1×10^{-5} mol L^{-1} of F^- ions (from a standard solution of TBAF), and 2×10^{-5} mol L^{-1} of receptor HL^1 in 4 : 1 DMSO–water. The UV-vis absorption spectrum of the resultant solution was measured and compared with the toothpaste-free F^- solution. As is shown in Fig. 6, the signal from the F^- contaminated toothpaste solution was stronger than that from the one without toothpaste which is ascribed to fluoride in toothpaste confirming that sensor HL^1 can be successfully employed for qualitative detection of F^- in toothpaste.

Construction of Logic Gates

As discussed above, the addition of F^- (3 equiv.) to HL^1 in DMSO resulted in a colour change from yellow to dark blue and emergence of a new absorption band at 600 nm, acting as ON behaviour. Subsequently, the F^- -induced chromogenic process

was fully reversed by the addition of trifluoroacetic acid (TFA), as a proton donor, acting as an OFF switch. Surprisingly, as illustrated in Fig. 7, these procedures could be repeated over several cycles which obviously manifest the high degree of reversibility. Overall, the results disclosed that the receptor HL^1 could be reused with proper treatment.

Encouraged by these observations, we further endeavoured to construct a molecular logic gate by using F^- and H^+ , from TFA, as two chemical inputs (In F and In T, respectively) and monitoring two different absorbances at 355 and 600 nm, as outputs. To elucidate the design of the logic gate, the inputs and optical outputs were coded with binary digits '0' and '1'. If we consider the absorbance at 355 nm as the output signal (Out1), an 'IMP' logic gate could be obtained at the molecular level, where the absorption was diminished only in the presence of fluoride ion (In F) but in all other circumstances, it remained in the ON state. Also, HL^1 can behave as an INHIBIT gate by monitoring the absorbance at 600 nm as another output (Out2).

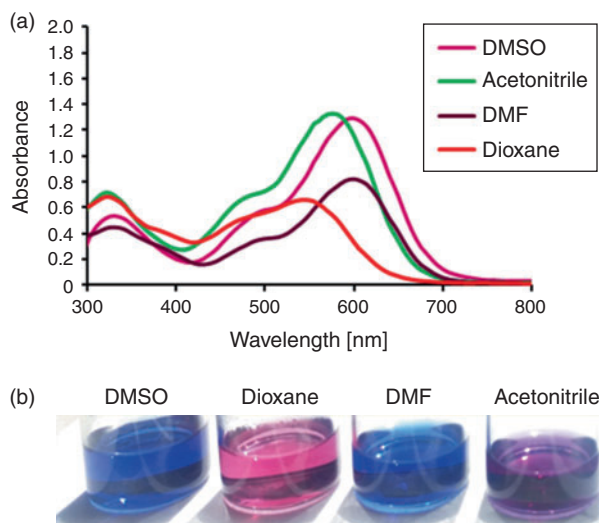
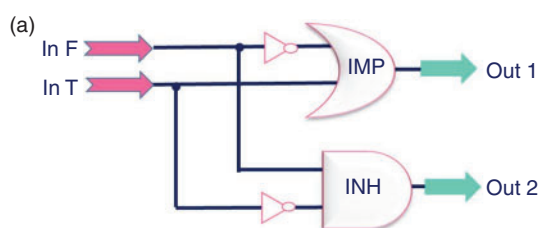


Fig. 5. (a) Changes in the UV-vis spectrum of HL^1 in various aprotic solvents upon addition of excess TBAF; (b) variable colour changes observed with the addition of F^- (3 equiv.) to the solutions of HL^1 in various polar aprotic solvents.

Table 2. Change in absorption maxima of HL^1 in different solvents on adding TBAF

Solvent	Dielectric constant	λ_{max} [nm]
1,4-Dioxane	2.21	545
Acetonitrile	35.49	545
Dimethylformamide	36.71	595
Dimethyl sulfoxide	46.8	600



In these circumstances, only when F^- is present, the absorption is '1' while the values of all other functions are '0'. Consequently, a complementary IMP/INH function could be interpreted with a single molecule and the logic circuit along with corresponding truth table are shown in Fig. 8a, b.

More interestingly, HL^1 can be offered as a potential 'Write-Read-Erase-Read' memory function through the absorption output signal at 600 nm as depicted in Fig. 9. In the current system, the ON state (Out2 = 1) is defined as the strong absorption at 600 nm, whereas the OFF state (Out2 = 0) corresponds to the weak absorption at identical wavelength. The two chemical inputs of F and TFA ions are designated In F and In T for the Set (S) and Reset (R), respectively. When the Set input is high (S = 1), the system writes and memorises the binary state '1'. Then, the stored information is erased by the Reset input (R = 1), resulting in the writing and memorisation of binary state '0'. These reversible and reconfigurable sequences of Set/Reset logic operations can be represented in the form of a feedback loop,

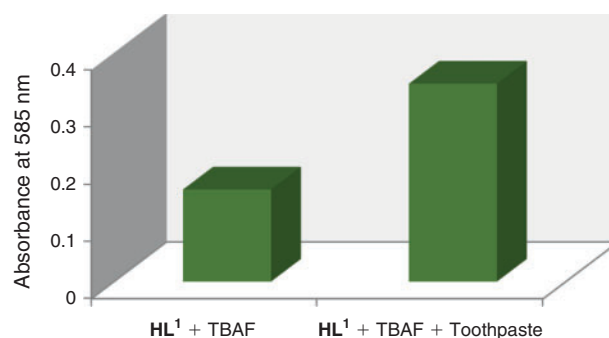


Fig. 6. The proof of concept for detection of fluoride in toothpaste: (left) HL^1 + TBAF; (right) HL^1 + TBAF + toothpaste.

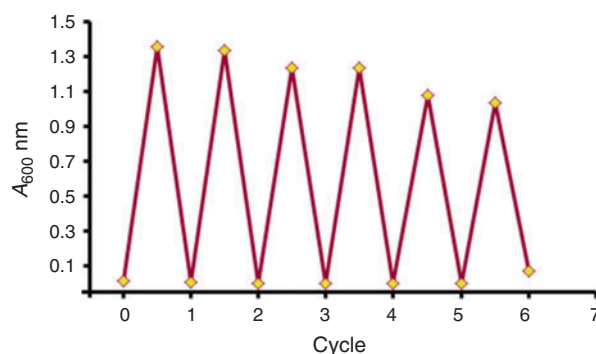


Fig. 7. Reversibility of the sensor HL^1 ($3 \times 10^{-5} \text{ mol L}^{-1}$) with sequential addition of F^- and TFA.

INPUTS		OUTPUTS	
In F	In T	Out 1 (355 nm)	Out 2 (600 nm)
0	0	1	0
0	1	1	0
1	0	0	1
1	1	1	0

Fig. 8. (a) The logic circuit and (b) the truth table for the complementary IMP/INH logic gate.

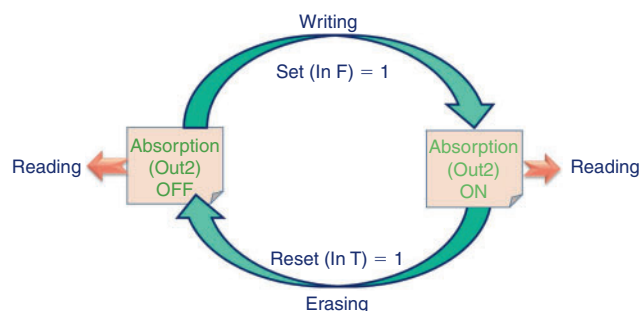


Fig. 9. The feedback loop exhibiting reversible logic operations with ‘Write–Read–Erase–Read’ function.

corroborating the memory feature with a ‘Write–Read–Erase–Read’ function through the output signal at 600 nm (Fig. 9).

Calculation Details

The molecular geometry of the receptors were fully optimised using the *Gaussian 09W* package at the B3LYP/6–311G (p, d) level. Vibrational frequency analysis, obtained at the same level, indicate that the optimised structures are at the stationary points corresponding to local minima without any imaginary frequency. Total energy and HOMO/LUMO energies of all the receptors, in the gas phase and in DMSO, were also examined. It is found that the enol–imine tautomer is energetically more

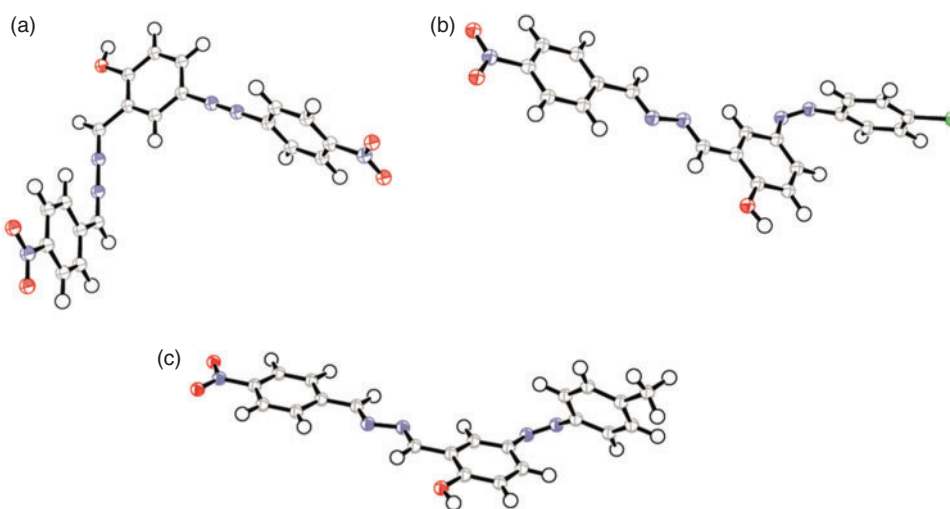


Fig. 10. The optimised geometry of enol–imine tautomer of the receptors: (a) HL^1 , (b) HL^2 , (c) HL^3 .

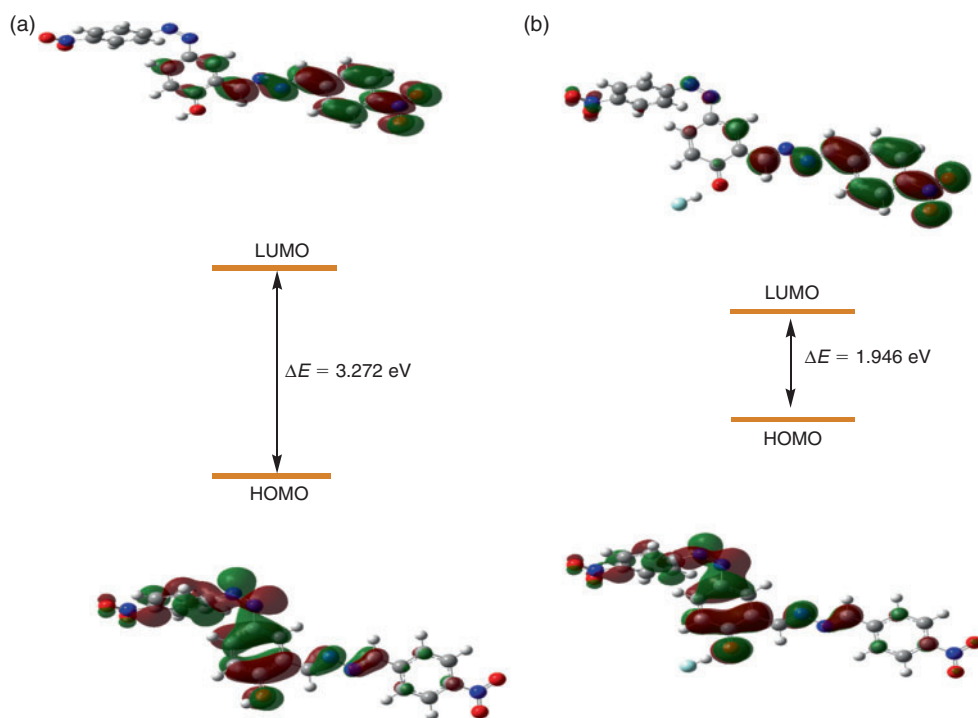


Fig. 11. HOMO–LUMO energy levels and the interfacial plots of the orbitals for (a) HL^1 and (b) the L^1 –F complex.

stable than the hydrazone form by ~ 303 (\mathbf{HL}^1), 309 (\mathbf{HL}^2), and 3 (\mathbf{HL}^3) kcal mol^{-1} . The optimised geometry of the enol-imine tautomer of the molecules and their complexes with F^- anions, in DMSO media, has been given in Fig. 10.

The orbital diagrams of the HOMO and LUMO of \mathbf{HL}^n ($n = 1-3$) were investigated (Fig. 10) (Supplementary Material). The energy gap between the HOMO and LUMO of \mathbf{HL}^1 , \mathbf{HL}^2 , and \mathbf{HL}^3 and their complexes with F^- , in DMSO, were 3.272, 3.022, and 2.863 eV and 1.946, 1.810 and 1.723 eV, respectively, reflecting substantial stabilisation due to complexation.

The HOMO of the receptors, before and after reaction with F^- , were more distributed on the 4-X-phenol-azo ($X = \text{NO}_2$, Cl and CH_3) moieties. However, after reaction with F^- the LUMO of the deprotonated species were located on the azo and 4-nitrobenzaldehyde moieties (Fig. 11). This indicated the binding of fluoride with \mathbf{HL}^1 due to the homogenisation of electron density through extended p-conjugation, which lead to the homogeneous distribution of electron density throughout the molecule.

The selected bonds length of \mathbf{HL}^1 and its complex, $\mathbf{L}^1\text{-F}$, are given in Table 3. The O-H bond distance in the $\mathbf{L}^1\text{-F}$ complex is 1.449 Å significantly longer than the O-H bond length (0.965 Å) of the free receptor. On the other hand, the C-O bond length in

the formed complex $\mathbf{L}^1\text{-F}$ is 1.275 Å which is shorter than the C-O bond length in the free receptor indicating development of a partial double bond character. This clearly indicated that deprotonation of \mathbf{HL}^1 by F^- occurred.^[7] The UV-vis frequency calculation of the $\mathbf{L}^1\text{-F}$ complex showed that \mathbf{HL}^1 can be characterised by absorption spectra exhibiting one intense band at ~ 600 nm, corresponding to the HOMO \rightarrow LUMO excitation. This absorption band agreed with that obtained experimentally at 595 nm. Visualisation of the UV-vis spectra of \mathbf{HL}^1 and the $\mathbf{L}^1\text{-F}$ complex was carried out using the *Chemission* program, <http://www.chemission.com> (Fig. 12).

The theoretical determination of thermodynamic parameters (ΔG , ΔH , and $T\Delta S$) and structural optimisation of \mathbf{HL}^1 with hydrated F^- anions provide further insight into the source of interactions between hydrated F^- ions with receptors in partial aqueous medium. The complexation of \mathbf{HL}^1 with F^- at 298 K gives $\Delta G = -5.42$ kcal mol^{-1} , $\Delta H = -1.36$ kcal mol^{-1} , and $T\Delta S = 4.06$ kcal mol^{-1} . The negative enthalpy and positive entropy changes indicated that binding between \mathbf{HL}^1 and F^- was created through hydrogen bonding and van der Waals interactions.^[46]

Conclusion

In the present work three new azo-azomethine receptors, \mathbf{HL}^n ($n = 1-3$), were synthesised via condensation reaction of 5-(4-X-phenyl)-azo-salicylaldehyde ($X = \text{NO}_2$, Cl and CH_3) **1-3** with (4-nitrobenzylidene)hydrazine precursors.

The receptor with a *p*- NO_2 substituent on the aromatic ring of the azo moiety (\mathbf{HL}^1) has excellent sensitivity and selectivity towards F^- in DMSO-water (4:1) solution. The ^1H NMR titration revealed that the colourimetric response was considered

Table 3. Calculated (B3LYP/6-311G (p, d)) of selected bond length of \mathbf{HL}^1 and its complex $\mathbf{L}^1\text{-F}$

Compound	Bond length [Å]	
	O-H	C-O
\mathbf{HL}^1	0.965	1.350
$\mathbf{L}^1\text{-F}$	1.449	1.275

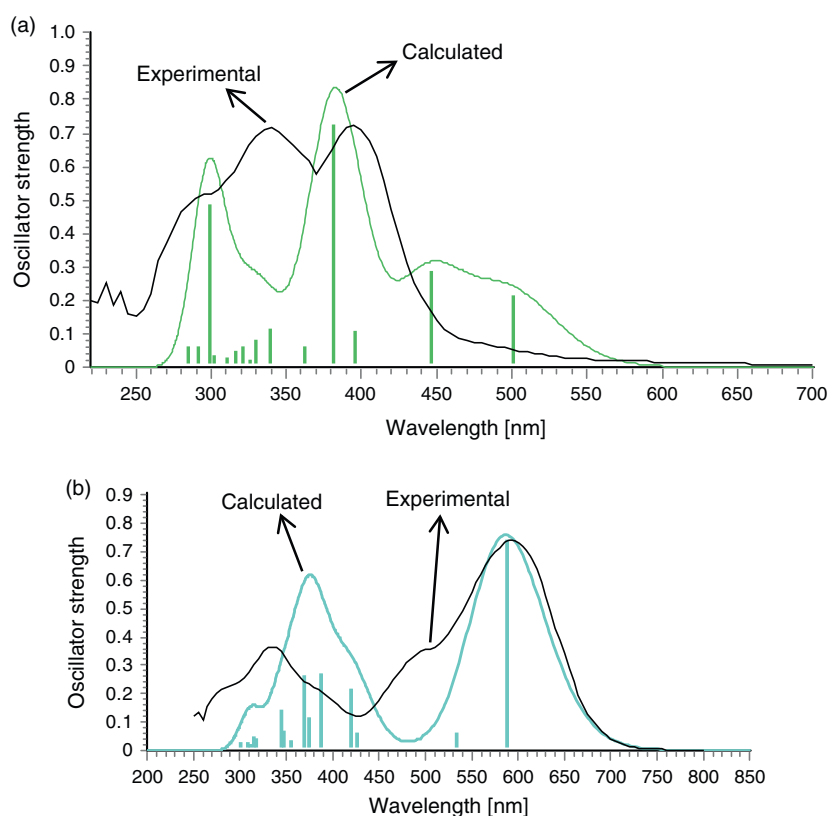


Fig. 12. Comparisons of (a) experimental and calculated absorption spectra of \mathbf{HL}^1 and (b) calculated absorption spectrum of the $\mathbf{L}^1\text{-F}$ complex.

to be the direct consequence of hydrogen-bond formation between phenolic groups of **HL**¹ and the fluoride ion followed by deprotonation. The mechanism of colourimetric sensing was corroborated by systematic DFT and TD-DFT calculations. Furthermore, based on the distinct reversibility of F⁻ with H⁺ as chemical inputs, **HL**¹ has also shown a reversible switching behaviour with complementary 'IMP/INH' logic function, which mimics the functions of a logic circuit displaying 'Write-Read-Erase-Read' behaviour possessing 'Multi-Write' ability.

Supplementary Material

Characterisation data of all compounds, NMR spectra, IR and UV-vis spectrophotometric titrations, stoichiometric determination by Benesi-Hildebrand method, Job's plot, and DFT data are available on the Journal's website.

Conflicts of Interest

The authors declare no conflicts of interest.

Acknowledgements

The authors express their gratitude to the Iran National Science Foundation (INSF) for financial support of this research (Grant No. 94015419).

References

- [1] P. A. Gale, N. Busschaert, C. J. E. Haynes, L. E. Karagiannidis, I. L. Kirby, *Chem. Soc. Rev.* **2014**, *43*, 205. doi:10.1039/C3CS60316D
- [2] H. J. Schneider, A. Yatsimirsky, *Chem. Soc. Rev.* **2008**, *37*, 263. doi:10.1039/B612543N
- [3] C. Caltagirone, P. A. Gale, *Chem. Soc. Rev.* **2009**, *38*, 520. doi:10.1039/B806422A
- [4] P. A. Gale, C. Caltagirone, *Chem. Soc. Rev.* **2015**, *44*, 4212. doi:10.1039/C4CS00179F
- [5] N. Busschaert, C. Caltagirone, W. V. Rossom, P. A. Gale, *Chem. Rev.* **2015**, *115*, 8038. doi:10.1021/ACS.CHEMREV.5B00099
- [6] X. F. Shang, *Spectrochim. Acta A* **2009**, *72*, 1117. doi:10.1016/J.SAA.2009.01.013
- [7] S. Vishwakarma, A. Kumar, A. Pandey, K. K. Upadhyay, *Spectrochim. Acta A* **2017**, *170*, 191. doi:10.1016/J.SAA.2016.07.021
- [8] T. B. Wei, H. Li, Q. Q. Wang, G. T. Yan, Y. R. Zhu, T. T. Lu, B. B. Shi, Q. Lin, Y. M. Zhang, *Supramol. Chem.* **2016**, *28*, 314. doi:10.1080/10610278.2015.1108419
- [9] D. Browne, H. Whelton, D. O'Mullane, *J. Dent.* **2005**, *33*, 177. doi:10.1016/J.JDENT.2004.10.003
- [10] Y. Ding, Y. Tang, W. Zhu, Y. Xie, *Chem. Soc. Rev.* **2015**, *44*, 1101. doi:10.1039/C4CS00436A
- [11] O. Barbier, L. Arreola-Mendoza, L.-M. Del Razo, *Chem.-Biol. Interact.* **2010**, *188*, 319. doi:10.1016/J.CBI.2010.07.011
- [12] P. T. C. Harrison, *J. Fluor. Chem.* **2005**, *126*, 1448. doi:10.1016/J.JFLUCHEM.2005.09.009
- [13] See p. 38 in: World Health Organization (WHO), *WHO Guidelines for Drinking-Water Quality* (4th edn) **2017** (WHO: Geneva).
- [14] M. Cametti, K. Rissanen, *Chem. Commun.* **2009**, 2809. doi:10.1039/B902069A
- [15] S. Erdemir, O. Kocyigit, O. Alici, S. Malkondu, *Tetrahedron Lett.* **2013**, *54*, 613. doi:10.1016/J.TETLET.2012.11.138
- [16] A. C. Gonçalves, N. C. Sato, H. M. Santos, J. L. Capelo, C. Lodeiro, A. A. dos Santos, *Dyes Pigments* **2016**, *135*, 177. doi:10.1016/J.DYEPIG.2016.02.032
- [17] V. Amendola, M. Bonizzoni, B. Esteban-Gomez, L. Fabbrizzi, M. Licchelli, F. Sancenon, A. Taglietti, *Coord. Chem. Rev.* **2006**, *250*, 1451. doi:10.1016/J.CCR.2006.01.006
- [18] T. Nishimura, S.-Y. Xu, Y.-B. Jiang, J. S. Fossey, K. Sakurai, S. D. Bull, T. D. James, *Chem. Commun.* **2013**, *49*, 478. doi:10.1039/C2CC36107H
- [19] L. Fabbrizzi, *Chem. Soc. Rev.* **2013**, *42*, 1681. doi:10.1039/C2CS35290G
- [20] H. Khanmohammadi, K. Rezaeian, *RSC Adv.* **2014**, *4*, 1032. doi:10.1039/C3RA42709A
- [21] A. K. Mahapatra, S. K. Manna, P. Sahoo, *Talanta* **2011**, *85*, 2673. doi:10.1016/J.TALANTA.2011.08.040
- [22] A. Kuwar, R. Patil, A. Singh, S. K. Sahoo, J. Marek, N. Singh, *J. Mater. Chem. C* **2015**, *3*, 453. doi:10.1039/C4TC02147A
- [23] D. Margulies, C. E. Felder, G. Melman, A. Shanzer, *J. Am. Chem. Soc.* **2007**, *129*, 347. doi:10.1021/JA065317Z
- [24] D. C. Magri, G. J. Brown, G. D. McClean, A. P. de Silva, *J. Am. Chem. Soc.* **2006**, *128*, 4950. doi:10.1021/JA058295+
- [25] S. Pramanik, V. Bhalla, M. Kumar, *ACS Appl. Mater. Interfaces* **2014**, *6*, 5930. doi:10.1021/AM500903D
- [26] N. Kaur, P. Alreja, *Tetrahedron Lett.* **2015**, *56*, 182. doi:10.1016/J.TETLET.2014.11.062
- [27] P. Ghosh, P. Banerjee, *Chem. Phys.* **2016**, *478*, 103. doi:10.1016/J.CHEMPHYS.2016.04.014
- [28] S. Sreejith, A. Ajayaghosh, *Indian J. Chem.* **2012**, *51*, 47.
- [29] S. Wang, G. Men, L. Zhao, Q. Hou, S. Jiang, *Sens. Actuators B* **2010**, *145*, 826. doi:10.1016/J.SNB.2010.01.060
- [30] H. Khanmohammadi, K. Rezaeian, *Spectrochim. Acta Part A* **2012**, *97*, 652. doi:10.1016/J.SAA.2012.07.013
- [31] M. J. Frisch, G. W. Trucks, H. B. Schlegel, G. E. Scuseria, M. A. Robb, J. R. Cheeseman, G. Scalmani, V. Barone, B. Mennucci, G. A. Petersson, H. Nakatsuji, M. Caricato, X. Li, H. P. Hratchian, A. F. Izmaylov, J. Bloino, G. Zheng, J. L. Sonnenberg, M. Hada, M. Ehara, K. Toyota, R. Fukuda, J. Hasegawa, M. Ishida, T. Nakajima, Y. Honda, O. Kitao, H. Nakai, T. Vreven, J. A. Montgomery, Jr, J. E. Peralta, F. Ogliaro, M. Bearpark, J. J. Heyd, E. Brothers, K. N. Kudin, V. N. Staroverov, R. Kobayashi, J. Normand, K. Raghavachari, A. Rendell, J. C. Burant, S. S. Iyengar, J. Tomasi, M. Cossi, N. Rega, J. M. Millam, M. Klene, J. E. Knox, J. B. Cross, V. Bakken, C. Adamo, J. Jaramillo, R. Gomperts, R. E. Stratmann, O. Yazyev, A. J. Austin, R. Cammi, C. Pomelli, J. W. Ochterski, R. L. Martin, K. Morokuma, V. G. Zakrzewski, G. A. Voth, P. Salvador, J. J. Dannenberg, S. Dapprich, A. D. Daniels, Ö. Farkas, J. B. Foresman, J. V. Ortiz, J. Cioslowski, D. J. Fox, *Gaussian 09, Revision B.01* **2009** (Gaussian, Inc.: Wallingford, CT).
- [32] I. I. R. Dennington, T. Keith, J. Millam, K. Eppinnett, W. L. Hovell, R. Gilliland, *GaussView, Version 3.09* **2003** (Semichem, Inc.: Shawnee Mission, KS).
- [33] C. Lee, W. Yang, R. G. Parr, *Phys. Rev. B* **1988**, *37*, 785. doi:10.1103/PHYSREVB.37.785
- [34] A. D. Becke, *J. Chem. Phys.* **1993**, *98*, 5648. doi:10.1063/1.464913
- [35] C. J. Cramer, *Essentials of Computational Chemistry: Theories and Models* (2nd edn) **2004** (Wiley: Chichester).
- [36] D. Pawlica, M. Marszałek, G. Mynarczuk, L. Sieroń, J. Eilmes, *New J. Chem.* **2004**, *28*, 1615. doi:10.1039/B409298H
- [37] H. Khanmohammadi, M. Erfantalab, *Spectrochim. Acta A* **2012**, *86*, 39. doi:10.1016/J.SAA.2011.09.053
- [38] G. Socrates, in *Infrared and Raman Characteristic Group Frequencies* (3rd edn) (Eds M. Brustolon, E. Giamello) **2001**, pp. 295–320 (John Wiley & Sons Ltd: Chichester, NY).
- [39] N. M. Rageh, *Spectrochim. Acta A* **2004**, *60*, 103. doi:10.1016/S1386-1425(03)00210-5
- [40] A. M. Khedr, M. Gaber, R. M. Issa, H. Erten, *Dyes Pigments* **2005**, *67*, 117. doi:10.1016/J.DYEPIG.2004.11.004
- [41] I. I. Abbas, H. H. Hammud, H. Shamsaldeen, *Eur. J. Chem.* **2012**, *3*, 156. doi:10.5155/EURJCHEM.3.2.156-162.542
- [42] R. S. Bhosale, M. M. A. Kelsonc, S. V. Bhosale, S. K. Bhargava, S. V. Bhosale, *Mater. Today: Proceedings* **2016**, *3*, 1883. doi:10.1016/J.MATPR.2016.04.088
- [43] H. A. Benesi, J. H. Hildebrand, *J. Am. Chem. Soc.* **1949**, *71*, 2703. doi:10.1021/JA01176A030
- [44] M. Boiocchi, L. Del Boca, D. E. Gómez, L. Fabbrizzi, M. Licchelli, E. Monzani, *J. Am. Chem. Soc.* **2004**, *126*, 16507. doi:10.1021/JA045936C
- [45] See pp. 550–552 in: C. Reichardt, T. Welton, *Solvents and Solvent Effects in Organic Chemistry* (4th edn) **2011** (Wiley-VCH: Weinheim).
- [46] P. D. Ross, S. Subramanian, *Biochemistry* **1981**, *20*, 3096. doi:10.1021/BI00514A017